This study investigates freight transportation process in the railroad network, which is formalized in the form of a train formation plan (TFP) as a complex dynamic system.

To assess the dynamic properties of a freight transportation model at the macro level of railroad system functioning, a method has been devised for analyzing the speed of transferring railroad car flows in the network. The proposed method reflects coordination dynamics not through the time of physical passage of trains in the network but through the ability of the system that organizes car flows into trains to quickly form a coherent state. The Kuramoto model was used to determine the speed of coordination. That has made it possible to distinguish TFP networks.

The application of the devised method and the simulation made it possible to compare the structural and dynamic properties of existing transportation system over the period from 2013 to 2019. The limited ability of TFP networks to global phase integration has been proven. It has been established that the TFP network in 2019 demonstrated a loss of systemic coherence, which is typical of decentralized point-to-point transportation networks. That was confirmed by calculating $\lambda_2^{2013} \approx 19.913342$ and $\lambda_2^{2019} \approx 0.497646$, where the difference between spectral gaps reached two orders of magnitude, while the time to reach the maximum of the order parameter r_{max} in 2019 was 4.07 times greater at comparable values of the order and $K_C = 6$. This indicates the transformation of the operating model from a centralized hub-and-spoke in 2013 to a more decentralized point-to-point model in 2019.

A special feature of the results based on the study is that the proposed method makes it possible to improve the quality of macroanalysis of changes in the structural and dynamic efficiency of the TFP network.

The scope of results practical application is the railroad industry. Conditions for the practical implementation of the findings are the importance of taking into account the results when analyzing operating TFPs

Keywords: Rail freight, railroad system, car flow, formation plan, hub-and-spoke, point-to-point, Kuramoto model

UDC 656.2

DOI: 10.15587/1729-4061.2025.341559

DEVISING OF A METHOD FOR ANALYSING THE PROPAGATION SPEED OF CAR FLOWS IN A TRAIN FORMATION PLAN BASED ON SYNCHRONISATION THEORY IN COMPLEX NETWORKS

Andrii Kyman
PhD, Associate Professor
Department of Cargo and Commercial Work Management*
Andrii Prokhorchenko
Corresponding author
Doctor of Technical Sciences, Professor
Department of Operational Work Management*
E-mail: andrii.prokhorchenko@gmail.com
Artem Panchenko
PhD, Associate Professor
Department of Theoretical and Applied Computer Science
V. N. Karazin Kharkiv National University
Svobody sq., 4, Kharkiv, Ukraine, 61022
Serhii Zolotarov
PhD Student
Department of Operational Work Management*
Mykhailo Kravchenko
PhD
Department of Transshipment and Fleet, Logistics Division
Kernel-Trade LLC
Taras Shevchenko lane, 3, Kyiv, Ukraine, 01001
Halyna Prokhorchenko
PhD, Associate Professor
Department of Operational Work Management*
Oleksandra Orda
PhD, Associate Professor
Department of Transport Technologies
Kharkiv National Automobile and Highway University
Yaroslava Mudroho str., 25, Kharkiv, Ukraine, 61002
*Ukrainian State University of Railway Transport
Oboronnyi Val sq., 7, Kharkiv, Ukraine, 61050

Received 24.07.2025
Received in revised form 29.09.2025
Accepted 06.10.2025
Published 31.10.2025

How to Cite: *Kyman, A., Prokhorchenko, A., Panchenko, A., Zolotarov, S., Kravchenko, M., Prokhorchenko, H., Orda, O. (2025). Devising of a method for analysing the propagation speed of car flows in a train formation plan based on synchronisation theory in complex networks. Eastern-European Journal of Enterprise Technologies, 5 (3 (137)), 56–67. https://doi.org/10.15587/1729-4061.2025.341559*

1. Introduction

In transportation systems, in particular railroad ones, it is critically important to systematically analyze changes in the transportation model since it is the change in service and operational rules that determines the routing of transport flows and the redistribution of the load on the network infrastructure. It is especially difficult to analyze the model of transportation

organization in railroad systems with predominantly freight traffic where there is no clear schedule of freight trains [1, 2]. Such freight railroads include the railroads in North America, India, China, Republic of Kazakhstan, and Ukraine [3–5]. The significant uncertainty of the transportation process in networks with predominantly freight traffic determines the need for macro-level approaches that make it possible to study the processes of transferring car flows not only according to a static scheme of directions but also as a dynamic process.

One of the key regulatory documents that defines the structural properties of the movement of car flows in freight railroad systems, in particular in Ukraine, is the Train Formation Plan (TFP) [6]. The TFP is introduced annually and significantly affects the economic and operational indicators of the railroad system from the use of capacity and the operation of marshalling yards to the reliability of logistics chains and the level of delay distribution. Analysis of changes in the TFP makes it possible to identify structural shifts in the logistics of transferring cars, assess the efficiency of marshalling yards, identify areas of increased risk of delays, and generally characterize the current operational model of the railroad system.

To study the processes of organizing car flows into trains, it is not enough to study only the topology of the network [7]; it is important to take into account its dynamic properties, in particular the speed of transferring car flows within the TFP. However, there are no methods that make it possible to assess the structural and dynamic efficiency of the TFP network and its change due to external factors (war, destruction of infrastructure, restructuring of routes).

Therefore, research into implementing new analysis methods based on the theory of synchronization in complex networks [8], which are capable of comparing alternative scenarios of railroad operation from the perspective of transportation process dynamics, is relevant.

2. Literature review and problem statement

Studies aimed at investigating transportation models in transport systems at the macro level have become important for determining the regularities of the functioning of infrastructure networks, assessing their properties, and predicting the impact of operational decisions on flow dynamics [9–12]. Paper [9] proposes, using the example of automobile traffic in cities, studying the structural properties of the infrastructure of the highway network in individual areas based on the macro-level dependence of traffic intensity on density based on the construction of a macroscopic fundamental diagram. It is shown that the aggregation of flows at the macro level provides correct network indicators suitable for the analysis of infrastructure solutions and traffic light synchronization. However, the research data cannot be transferred to rail transport, where the flows of cars are reshaped at support stations and have different parameters and traffic restrictions.

In [10], approaches to the calibration and validation of macroscopic traffic models for large motorway networks were reviewed. The effectiveness of analysis methods from the position of the macro level of the functioning of the transport network was confirmed. However, the issues related to the transfer of this approach to railroad systems with network plans of car movements, spatially heterogeneous operating conditions of stations and taking into account the speed of the system entering the agreed mode remained unresolved.

Studies [11, 12] emphasize the importance and value of research aimed at analyzing demand and flows at the macro level of freight systems. However, the authors do not pay attention to the analysis of car flow movements on the railroad network.

Work [13] confirms the effectiveness of the macro-level approach to the analysis of the railroad system. It is proposed to combine micro-details of operation into aggregated network indicators for assessing throughput using Petri nets. However, the research data are applied to railroads with cyclic schedules, which do not include freight railroads.

In [14], a simulation macro model of the grain supply chain on international routes with the distribution of freight transportation between railroads and road transport was built. The proposed model makes it possible to assess the consequences of delivery delays but does not make it possible to assess the dynamic macro properties of the entire transport system.

An important direction for devising macroanalysis methods is to pay attention to studying the coherence and stability of dynamic processes in transport networks based on the theory of synchronization of complex systems. Works [15, 16] consider the modeling of transport flows using approaches to the analysis of coherence and phase transitions in dynamic networks. One of the most common mathematical models used in this area is the Kuramoto model [17], which makes it possible to describe the processes of phase coordination between system elements. It has been applied in studies of road transport for self-synchronization of speeds and "dilution" of the phases of transport waves at intersections in V2X networks, which reduces delays and fuel consumption, and also increases network traffic coordination [18].

In public transport, the phenomenon of bus bunching is described as the phase synchronization of a ring of interacting oscillators, which gives critical thresholds of demand and policies to prevent traffic asynchrony, which are interpreted through synchronization mechanisms [16]. However, there are no examples of the application of the Kuramoto model to the study of freight railroads.

For the railroad system, the possibility of analyzing the dynamic properties of the transport process based on phase synchronization in schedules as a network property has been shown, which opens the way to coherence metrics for planning and assessing stability [19]. The studies described above demonstrate applicability of the synchronization paradigm to the task of studying operational logistics. However, most of the scientific works have focused on the study of transport processes specific to the relevant transport network and cannot be applied to freight railroad systems.

The issue of analyzing the speed of processes using the Kuramoto model in transport systems has been studied to a much lesser extent. Available papers consider the speed of the system entering the synchronization mode [20, 21] but this aspect has been studied mainly in the context of theoretical physics and general network systems. For transport systems, and especially for railroad systems, there are no examples of applying the Kuramoto model specifically for analyzing the speed of flow transfer in transportation plans. Known studies analyze the Train Formation Plan or similar structures of train flow movement from the standpoint of statistical characteristics of the topology [22] rather than the dynamics of coordination. Thus, despite studies on the application of synchronization theory and the Kuramoto model in transport systems, the problem of quantifying the speed of transfer of car flows in the train formation plan remains insufficiently examined.

Therefore, the task to devise a method that would provide a quantitative assessment of the dynamics of coordination and transfer speed of car flows in complex railroad networks, taking into account the specificity of their functioning without reference to freight train schedules, remains unresolved.

3. The aim and objectives of the study

The purpose of our study is to devise a method for analyzing the speed of carriage flow propagation in a train formation plan based on the theory of synchronization in complex networks. This will make it possible to identify transportation models, quantitatively assess the dynamics of railroad network coordination, and compare different versions of TFPs.

To achieve this goal, the following research tasks were set:

– to determine the structure of the method for analyzing the speed of carriage flow propagation in a train formation plan, which is based on the formalization of the dynamics of coordination of the stations in the network;

– to conduct a comparative analysis of the speed of carriage flow propagation when changing the network topology in the period from 2013 to 2019 and to investigate the impact of changes in the TFP structure on the coherence and stability of the functioning of the railroad network as a whole.

4. The study materials and methods

The object of our study is the process of transferring car flows in the railroad network, formalized in the form of a train formation plan as a complex dynamic system.

The principal hypothesis of the study assumes that increasing the efficiency of a railroad system is possible through the identification and quantitative description of the dynamics of transferring car flows in the TFP network, as well as changes in the structural and dynamic properties of the transportation model at the macro level. For this purpose, an assessment of the structural and dynamic efficiency of the TFP network is provided based on quantitative measurement of the speed of coordination of the network elements and determination of the characteristics of the transportation model that affect the dynamics of freight car transfer. This task can be solved by devising a method that combines spectral, dynamic, and architectural analysis of TFP graphs and makes it possible to compare alternative versions of the train formation plan from the standpoint of their ability to ensure the stability and coherence of the transportation process.

One of the key characteristics of complex transport systems is the ability of their subsystems to work in synchronization [8]. In the context of railroad networks, synchronization is associated with the ability of the system to respond to changes in train traffic, promptly coordinate the actions of nodes that are sorting or district stations within the boundaries of the TFP assignments. For modeling such processes, the Kuramoto model [17] is effective, which makes it possible to explore the dynamic properties of connected graphs that describe the structure of a transport network, in particular a railroad one.

In the Kuramoto model, the nodes of the graph are interpreted as oscillators with individual natural frequencies, and the edges of the graph as couplings that determine the degree of mutual influence between the nodes [17, 23]. Our study uses the methodology described in [7], which involves representing information in the TFP document in the form of a directed graph $G(V, E)$. In $G(V, E)$, the vertices are railroad stations, and the arcs correspond to the planned directions of movement of cars in trains, which are termed TFP destinations. Our study proposes testing the devised method by performing a comparative analysis of TFP network graphs of different years.

According to the information from two regulatory documents [6], the TFPs of 2012–2013 and the TFPs of 2018–2019 were processed and graphs were constructed, which are designated as G2013 and G2019, respectively. For each graph, the largest strongly connected component (SCC) was selected, which guarantees the presence of a closed loop of excitation transfer between all stations and allows for the correct use of spectral methods. Graph structures and calculations were performed using the NetworkX library in Python. The visualization of SCC graphs is shown in Fig. 1.

In the context of studying the operational model of freight transportation in the railroad system, each vertex i of graph $G(V, E)$ is interpreted as a technical station on the network included in the TFP. Technical stations perform the functions of coordinating the intensity of the transfer of car traffic according to the corresponding TFP assignments, and phase $\theta_i(t)$ describes the state of its coordination with other technical stations of the network. This can be interpreted as the state of readiness of the station to transfer or receive car traffic, and the synchronization speed reflects how quickly the entire network coordinates its actions to transfer car traffic in a train formation plan. The evolution of the phases is given by the equation given below [24]

$$\frac{d\theta_i}{dt} = \omega_i + \frac{K}{N}\sum_{j=1}^{N} A_{ij}\sin\left(\theta_j - \theta_i\right), \quad (1)$$

where A_{ij} is the adjacency matrix of the graph; ω_i are the natural frequencies measured through the natural frequency; K is the coupling coefficient (the coupling strength parameter). Numerical integration is performed by the Euler method [25] at a fixed step Δt, and initial values $\theta_i(0) \sim U[0, 2\pi)$ and $\omega_i(0) \sim U[a, b)$ make it possible to model stochasticity in the railroad system operation.

The synchronization state of the entire network is described by the order parameter $r(t)$, which reflects the degree of coherence between the phases

$$r\left(t\right) = \left|\frac{1}{N}\sum_{j=1}^{N} e_i^{\theta_j(t)}\right|. \quad (2)$$

The maximum value $r_{\max}$ in the simulation process is interpreted as the network's ability to achieve global synchronization. To eliminate the large-scale influence of different graph topologies, connectivity parameter K was normalized by the following formula

$$K = \left|\frac{\langle k\rangle}{N}\right|, \quad (3)$$

where $\langle k\rangle$ is the average degree of the graph; N is the total number of vertices of the graph. This approach provides a fair comparison between graphs of different density of couplings.

Fig. 2 shows an example of a visual representation of phase angles at the vertices of the graph in a TFP network.

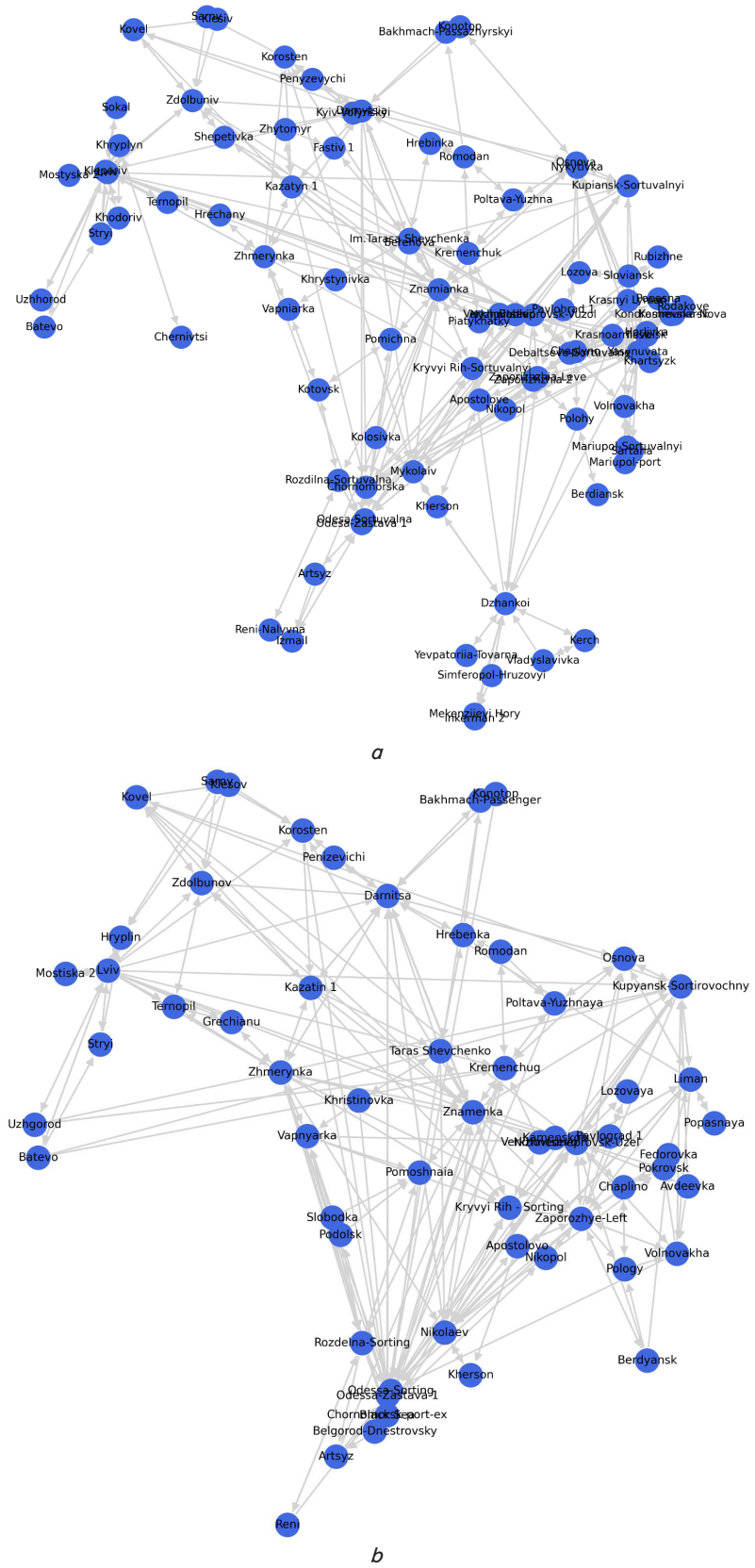

a

b

Fig. 1. Visualization of the largest strongly connected component of the network of train formation plan assignment graphs: *a* – G2013; *b* – G2019

The slope of the oscillator arrow in the Kuramoto model on the graph corresponds to phase angle θ_i of each node i at time t. This is a key component of the model dynamics. The phase θ_i is defined in radians within $[0, 2\pi)$. The arrow from the node center in the direction of the angle indicates the direction of the "oscillation vector" or the direction in which the node "rotates" in phase space, where $(x, y) + (\cos(\theta_i), \sin(\theta_i))$. Accordingly, nodes with the same or close phases have parallel arrows. This can be interpreted as the position of a pendulum synchronized with others.

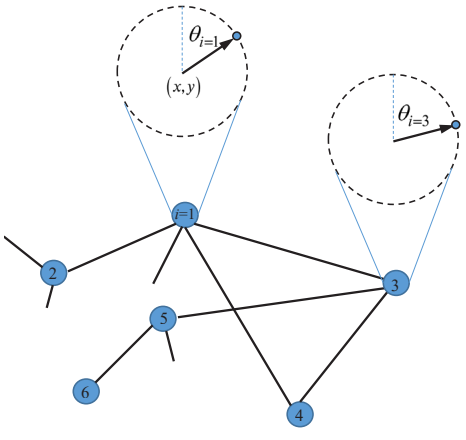

Fig. 2. Schematic representation of a fragment of the train formation plan graph with the slope of the oscillator arrows in the Kuramoto model

To provide a new level of formalized analysis of TFP, our study proposes integrating the dynamic approach based on the Kuramoto model with spectral analysis. Below is a methodology for determining the ability of the TFP network to synchronize based on spectral analysis.

The key result of the Kuramoto theory is the phase transition to synchronization that occurs when the critical coupling strength K_C is reached. The critical coupling strength K_C defines the minimum level of coherence between vertices in a network at which a system can effectively self-coordinate. This is fundamentally important in assessing how much "coupling" or "interaction intensity" is needed to achieve synchrony in complex systems [26]. An illustration for an arbitrary system of the phase transition to synchronization that occurs when the critical coupling strength K_C is reached is shown in Fig. 3 [26].

For graphs with a symmetric structure and uniform frequency distribution, the critical value can be approximately determined as

$$K_C \approx \frac{2\Delta\omega}{\lambda_2}, \quad (4)$$

where $\Delta\omega$ – width of the frequency range $\Delta\omega = \omega_{\max} - \omega_{\min}$ (for example, we can assume that $\Delta\omega \in [0.5, 1.5] \Rightarrow \Delta\omega = 1.0$); λ_2 – second eigenvalue of the Laplacian of the graph (spectral gap).

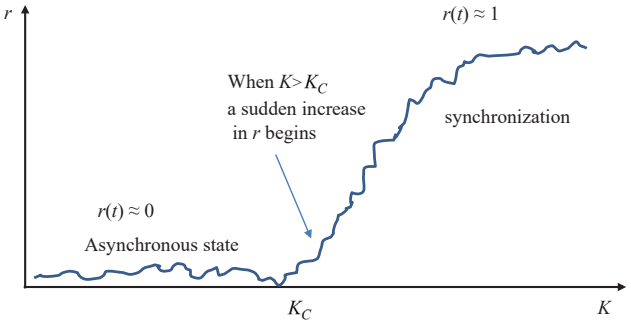

Fig. 3. Plot of change in the order parameter depending on coupling strength [26]

Excessive decentralization (low K) makes the system chaotic, while it is important to find the critical point K_C, after which the system abruptly switches to phase ordering. Knowing the optimal level of communication in the system makes it possible to achieve stable synchronization, where the PFT has a coordinated processing and movement of train flows in the railroad network.

5. Results of devising a method for analyzing the transfer speed of car flows in a train formation plan

5. 1. Structure of the method for analyzing the transfer speed of car flows in a train formation plan

5. 1. 1. Spectral assessment of network synchronization ability

To provide a new level of formalized analysis of TFP, it is proposed to integrate a dynamic approach based on the Kuramoto model with spectral analysis. In order to assess the synchronization potential of the TFP topology, an approach based on spectral analysis of the Laplace graph matrix [27] was applied. Spectral assessment of synchronization ability. In addition to dynamic modeling, the network synchronization ability can be theoretically assessed through spectral properties of the graph. In particular, consideration of the eigenvalues of a Laplace matrix [27]

$$L = D - A, \tag{5}$$

where D is the diagonal matrix of vertex powers; A is the adjacency matrix.

Let $0 = \lambda_1 < \lambda_2 \le ... \le \lambda_N$ be the eigenvalues of L. The $\Delta\lambda = \lambda_2 - \lambda_1 = \lambda_2$ quantity is known as the spectral gap (algebraic connectivity) and serves as a criterion for the stability of the synchronous state (the larger λ_2, the faster the system stabilizes after a perturbation), the rate of achieving coherence in cases of strong coupling $K \gg 1$. In the context of the Kuramoto model, a larger spectral gap means a better ability of the network to achieve a synchronous state at a fixed noise level and natural frequency spread.

Taking into account the fact that graphs are directed while the classical Laplace matrix L is generally unsuitable for such topologies, an assumption was adopted about the approximate symmetry of the largest SCC. This makes it possible to interpret the calculation of the spectral gap as a heuristic indicator of the network's ability to coherent dynamics.

The spectral gap was determined as the difference between the second and first non-zero eigenvalues of the Laplace matrix [27]

$$\Delta\lambda = \lambda_2 - \lambda_1, \tag{6}$$

where λ_1 is the first non-zero eigenvalue of the Laplace matrix; λ_2 is the second non-zero eigenvalue of the Laplace matrix.

According to synchronization theory, this indicator serves as an approximate numerical indicator of how quickly the network is able to transition to a coherent or so-called synchronized state within the framework of a Kuramoto-type model. In this case, a larger spectral gap corresponds to a higher stability of the synchronous state but may be accompanied by a slower transition to it.

5. 1. 2. Formalization of the method for analyzing the speed of carriage flow transfer based on the theory of synchronization in complex networks

For a comparative assessment of the speed of coordination of the railroad network in terms of carriage flow transfer in the process of train formation, it is proposed to formalize the method in the form of a diagram of the sequence of stages of its implementation. The sequence of stages reflects the process of formalizing the dynamics of carriage flow transfer in the train formation plan based on the theory of synchronization of network structures. Within the framework of the formalization, dynamic modeling based on the theory of synchronization and spectral analysis of the topological properties of the graph of the train formation plan are combined. In the proposed idea of formalization, the speed of carriage flow transfer is compared not directly through the time of physical passage of the train between the TFP stations but indirectly based on studying the ability of the system for organizing carriage flows into trains to synchronize. This reflects the effectiveness of coordination of actions between stations in the train formation plan.

Within the formalization of the method, the rate of transfer of car flows is interpreted as the rate of achieving coordinated behavior in the network, which is modeled through the rate of growth of the order parameter $r(t)$, the determination of the spectral gap λ_2 and the critical coupling strength K_C of the two graphs under study. This makes it possible to compare the networks of the hub-and-spoke versus point-to-point operational model [28] in terms of the efficiency of station coordination, which in the real context corresponds to the speed and reliability of the transfer of car flows in the TFP.

To obtain a quantitative characteristic of the dynamics of transportation system behavior, it is proposed to determine the synchronization rate or the average increase in the order parameter $r(t)$ in the time interval where the most active growth of coherence occurs, i.e., in the transition zone from an uncoordinated to a partially or fully synchronized state

$$\Delta r = \frac{r(t_2) - r(t_1)}{t_2 - t_1}, \tag{7}$$

where t_1, t_2 are the beginning and end of the transition interval, which are selected according to the criterion of growth of $r(t)$; t_1 is the time point when $r(t)$ first exceeds $0.1 \cdot r_{\max}$, i.e., exceeds the value of 10% of the maximum; t_2 is the time point when maximum $r_{\max} = r(t_2)$ is first reached. Δr is an indicator of the speed of phase matching between the nodes of the graph. The transition zone is estimated by the relative increase. It should be noted that in the case of a slight increase in $r(t)$, when $r(t_2) - r(t_1) < 0.2$, indicator Δr can be interpreted as an indicator of inertia or network insensitivity to synchronization. In addition to Δr, it is proposed to determine the

time t of reaching the critical coherence threshold value r_{max}. These indicators make it possible to distinguish TFP networks that have the same r_{max} but reach it at different speeds. Fig. 4 shows a scheme of the method for comparative analysis of the speed of transfer of car flows in the train formation plan based on the theory of synchronization in complex networks.

According to the scheme in Fig. 4, at the first stage, the graphs of the train formation plan for different years are loaded. The connectivity and absence of isolated nodes are checked. Next, the most strongly connected component of each graph is selected, which is a necessary condition for ensuring the connectivity of the model and its subsequent spectral analysis. After that, the SCC size is calculated as the number of its vertices (Stage 2).

At the third stage, the spectral gap is calculated as the second non-zero eigenvalue of the normalized Laplace matrix. This indicator serves as an assessment of the network's ability to synchronize, where larger values correspond to more stable coordination of the dynamics between nodes.

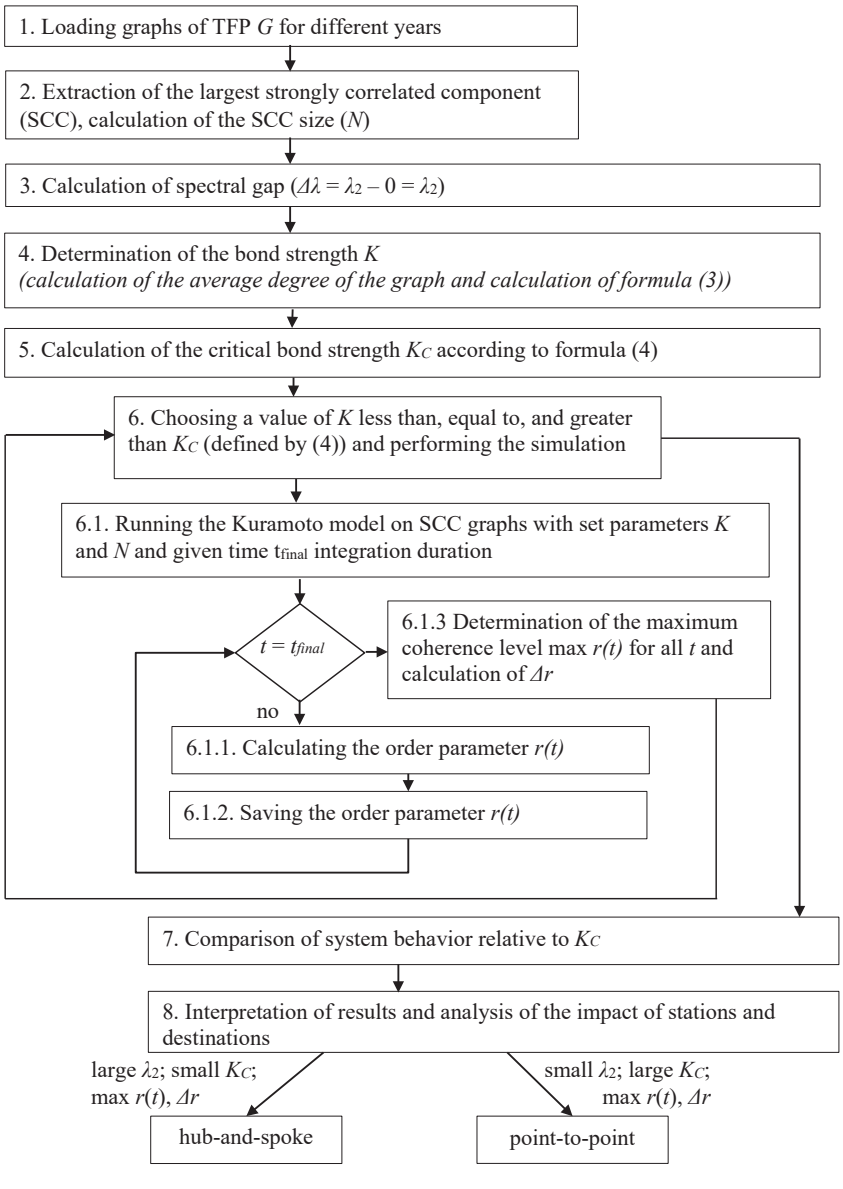

Fig. 4. Scheme of the method for comparative analysis of the speed of transfer of car flows in a train formation plan based on the theory of synchronization in complex networks

At the fourth stage, the coupling strength between nodes is determined, which models the degree of mutual influence of stations in the system, using a formula based on the average degree of the graph (3). This allows for correct scaling of the interaction in the model. The fifth stage involves calculating the critical coupling strength according to formula (4), which takes into account the spectral properties of the network and its size. This indicator determines the threshold at which synchronization can occur in the system.

At the sixth stage, the simulation is carried out for different values of the coupling strength K. It is proposed to simulate at the values of coupling strength K that are determined by the topological properties of each network according to formula (3). In addition, with K less ($K = 0.5\,K_C$), equal ($K = K_C$), or greater ($K = 2K_C$) than the critical value (K_C is calculated from formula (4)). This allows for the presence of a phase transition to a state of coherence to be detected. The simulation of the Kuramoto model on the SCC of each TFP graph is performed with a given coupling strength parameter K, the number of nodes in the SCC N, and the simulation time horizon t_{final}. Within the simulation stage, the order parameter is calculated as a global indicator of the level of phase coordination between nodes, its values are stored, and the maximum coherence level is determined throughout the simulation period, Δr is calculated using formula (7). The seventh stage includes a comparison of the dynamics of the order parameter for graphs of different years, taking into account the critical coupling strength, which makes it possible to assess the network's ability to quickly coordinate when transferring train traffic.

The final stage is the interpretation of the results obtained, which makes it possible to identify structural differences between the models. In particular, SCC TFP graphs with a larger spectral gap and a lower critical coupling strength are characterized by a more centralized hub-and-spoke type hub structure. Graphs with less synchronization ability exhibit characteristics of a decentralized point-to-point routing model.

5. 2. Results of comparative analysis of the speed of carriage flow propagation in a train formation plan

According to the proposed structure of the method and the developed program in the Python environment, simulation was performed for two SCC graphs under different conditions for setting the value of K according to stage 6 of the method (Fig. 4). For the first run of the simulation, the so-called eigenvalues K of each SCC graph were used, which are determined by the topological properties of each subnet. According to formula (3), the eigenvalue of the corresponding SCC by the average degree is $K_{SCC}^{G2013} = 0.0866$ and $K_{SCC}^{G2019} = 0.1672$, respectively. The critical values of K_C should be calculated

immediately. Therefore, provided that the graph is connected, and in the TFP of each year an SCC is distinguished, then the spectral gap is defined as the minimum non-zero eigenvalue of the Laplace matrix, i.e., at $\lambda_1 = 0$, the spectral gap is the second eigenvalue of the Laplace matrix. Thus, a smaller value of λ_2 means a higher critical interaction strength required to achieve synchronization, which is typical for sparse or weakly connected networks, such as the G2013 and G2019 TFP networks. For the SCC of the G2013 graph, given $\Delta\omega \in [0.5, 1.5] \Rightarrow \Delta\omega = 1.0$ and the found $\lambda_2^{2013} \approx 19.913342$, and therefore the critical value can be approximately determined as

$$K_C^{G2013} \approx \frac{2 \cdot 1}{19.913342} \approx 0.10.$$

Under the same conditions and the found $\lambda_2^{2019} \approx 0.497646$, critical value for the SCC of graph G2019 is calculated as

$$K_C^{G2019} \approx \frac{2 \cdot 1}{0.497646} \approx 4.02.$$

The final simulation time t_{final} should be chosen taking into account the duration of transients in the system and ensuring that the order parameter $r(t)$ reaches a plateau under most regimes [29]. In our study, the final t_{final} value was determined based on the results of test runs, which showed that 500 simulation steps are sufficient to study the basic properties of network synchronization. The determined simulation duration is typical practice for medium-sized networks. The evolution of synchronization of two SCC of graphs at K, which is determined from formula (3), is shown in Fig. 5. Table 1 gives the simulation results obtained. In the SCC of G2013 network, the coupling strength $K_{SCC}^{G2013} = 0.0866$ is close to critical $K_l^{G2013} \approx 0.10$, which indicates the relative structural stability of the subgraph. In the SCC of G2019, on the contrary, there is a very large discrepancy between $K_{SCC}^{G2019} = 0.1672$ and $K_C^{G2019} \approx 4.02$, which indicates greater decentralization.

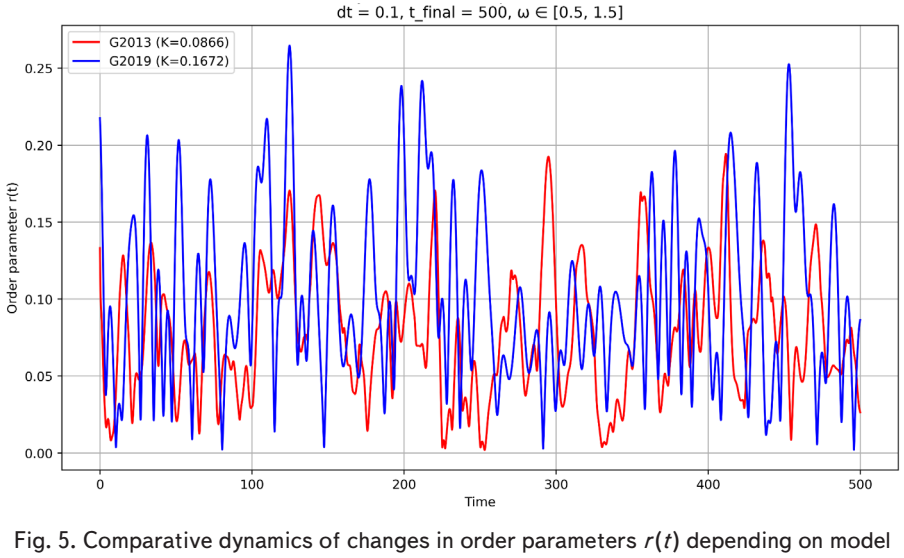

Fig. 5. Comparative dynamics of changes in order parameters $r(t)$ depending on model time of strongly connected components of two graphs G2013 and G2019 at their eigenvalues K

According to the results in Table 1, synchronization is slow in G2013, reflecting a complex and centralized topology that provides robust global coordination. The higher synchronization speed in G2019 ($\Delta r = 0.000378$) may seem positive but the synchronization of the system may occur at a local rather than global level. The G2019 network is less dependent on hubs but may be more vulnerable to the failure of individual links.

Table 1

Estimated SCC synchronization rates of two graphs G2013 and G2019 at their eigenvalues K

Indicator	G2013	G2019
SCC size	89	60
Spectral gap λ_2	19.913342	0.497646
The power of coupling K	0.086605	0.167222
The critical power of coupling K_C	0.100435	4.018918
r_{max}	0.194367	0.264661
Time r_{max}	411.600000	124.700000
Start of the transition zone $r(t)$	0.133171	0.217580
End of the transition zone $r(t)$	0.194367	0.264661
Start of the transition zone t	0.000000	0.000000
End of the transition zone t	411.600000	124.700000
Synchronization rate Δr	0.000149	0.000378

Considering that at the eigenvalues of coupling strength K both subnetworks are far from global synchronization, it is important to investigate the processes at $K \approx K_C$. Comparative graphs of the dynamics of changes in the order parameters $r(t)$ depending on the model time SCC of the two graphs G2013 and G2019 at $K \approx K_C$ are shown in Fig. 6. The simulation results are given in Table 2.

According to Table 2, SCC G2013 at $K \approx K_C$ compared to condition $K < K_C$ has a reduction in the time to reach the maximum r_{max} from 411.6 (Table 1) to 256 steps. The maximum synchronization indicator increases, and the rate Δr increases almost 5 times, which indicates that the system has acquired high global coherence. Therefore, it can be stated that when the critical strength of the coupling is reached, G2013 sharply activates global synchronization. This is typical for centralized systems with effective information propagation through hubs. In the SCC of G2019 at $K \approx K_C$ compared to condition $K < K_C$, on the contrary, r_{max} decreases from 0.265 to 0.171, that is, synchronization worsens, even under conditions of formal achievement of the critical level of coupling. The synchronization rate Δr slows down from 0.000378 to 0.000636. The time to reach the maximum r_{max} remained almost unchanged. The G2019 network does not show a significant increase in synchrony, which indicates the absence of centralized couplings.

The obtained spectral gap $\lambda_2 = 0.497646$ indicates a low level of structural integration, which indicates the importance of this indicator for achieving consistency of operations in the railroad system. Without structural integration, the critical

value of coupling does not guarantee consistency of actions in the system.

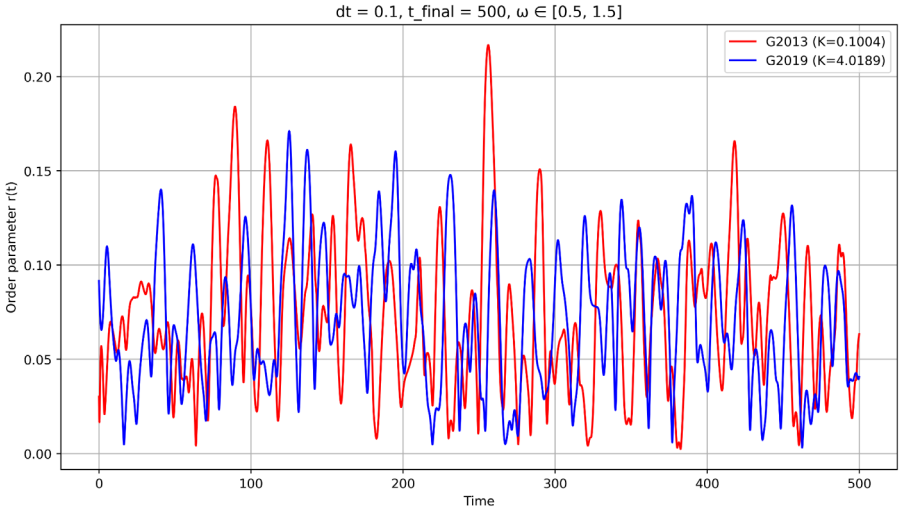

Fig. 6. Comparative dynamics of change in order parameters $r(t)$ depending on model time of the strongly connected component of two graphs G2013 and G2019 at $K \approx K_C$

Table 2

Estimated SCC synchronization rates of two graphs G2013 and G2019 at $K \approx K_C$

Indicator	G2013	G2019
SCC size	89	60
Spectral gap λ_2	19.913342	0.497646
The power of coupling K	0.100435	4.018918
The critical power of coupling K_C	0.100435	4.018918
r_{max}	0.216829	0.171119
Time r_{max}	256.000000	125.100000
The start of transition zone $r(t)$	0.030257	0.091590
The end of transition zone $r(t)$	0.216829	0.171119
Start of transition zone t	0.000000	0.000000
The end of transition zone t	256.000000	125.100000
Synchronization rate Δr	0.000729	0.000636

To study the synchronicity properties of the subgraphs of the compared TFP networks, it is important to perform a phase analysis. To find the dependence of the order parameter on the strength of the coupling, it is proposed to conduct a simulation according to the Kuramoto model within the range of values of coupling strength $K \in [0.01, 15]$. This will make it possible to calculate the average value of the order parameter $r(t)$ for each subgraph. The average value of the order parameter is taken to take into account the stationarity (quasi-stationarity) of the regime for each K. This corresponds to the generally accepted practice in network coherence studies [30]. The resulting phase diagram of synchronization is shown in Fig. 7.

According to our analysis of the diagram in Fig. 7, for both SCC of TFP graphs, the order parameter varies within 0.08–0.11 over the entire range $K \in [0.01, 15]$. Such values are less than 0.2, which proves the low ability of the networks to synchronize. This is typical for complex and fragmented networks, which include the TFP network. In the SCC of G2013, the critical value is quite small $K_C^{G2013} \approx 0.10$, in terms of its own characteristics, and after $K \geq 6$, reaching the level of 0.11, the order parameter $r(t)$ stops growing. In the subsequent dynamics of change in the value of $r(t)$ can be considered as reaching a plateau, where the network is "saturated" with local coherent groups, but is not able to "transition" to global coherence. Given that the order parameter $r(t)$ does not reach 1, global synchronization does not occur. It can be concluded that SCC in the TFP graphs retains fragmentation, even with a high coupling strength.

In the SCC of G2019, the graph has a different dependence: at $K = 0.01$, it has the largest average value of the order $r(t) = 0.13$, which decreases to a critical level with outliers, and at $K = 4.74$, it has an average $r(t) = 0.078$. A sharp decrease in $r(t)$ is observed when displaying pronounced jumps. This behavior indicates the disintegration of phase clusters, which can be associated with the structural fragmentation of the TFP network. Further, at $K \geq 4$, significant fluctuations are observed with a general trend of decreasing $r(t)$. This is a sign that the network is becoming disjointed, where some stations form small coherent clusters, but the entire network is not globally synchronized. Jumps in $r(t)$ often indicate the presence of "structural holes", i.e., weak components or insulator nodes that interfere with the propagation of phase to the entire network. As the network grows, it becomes even more "fragmented". This indicates excessive dynamic instability to global coherence. It can be assumed that the SCC of G2019 topology does not have a "core" that could "pull" all nodes to a common phase. The network contains many end stations, "detached" branches, or nodes with low connectivity. This confirms the decrease in the ability of the G2019 graph to synchronize compared to G2013.

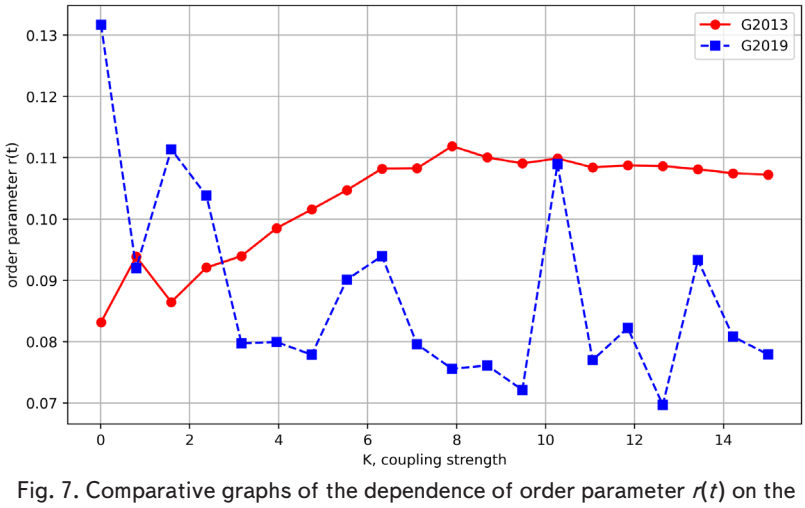

Fig. 7. Comparative graphs of the dependence of order parameter $r(t)$ on the strength of coupling for the SCC of two graphs G2013 and G2019 ($t_{final} = 500$)

As part of the study of the synchronization properties of the largest strongly connected component of the G2013 and G2019 graphs, it is proposed to consider the supercritical coupling strength regime, when the parameter value is set at $K = 6$, which significantly exceeds the critical threshold values for both networks. This approach makes it possible to assess the network's potential for deep synchronization under conditions of maximum node interaction and to identify hidden structural differences between the networks. Comparative plots of the dynamics of change in the order parameters $r(t)$ depending on the model time of SCC of the two graphs G2013 and G2019 at $K = 6$ are shown in Fig. 8. The simulation results are given in Table 3.

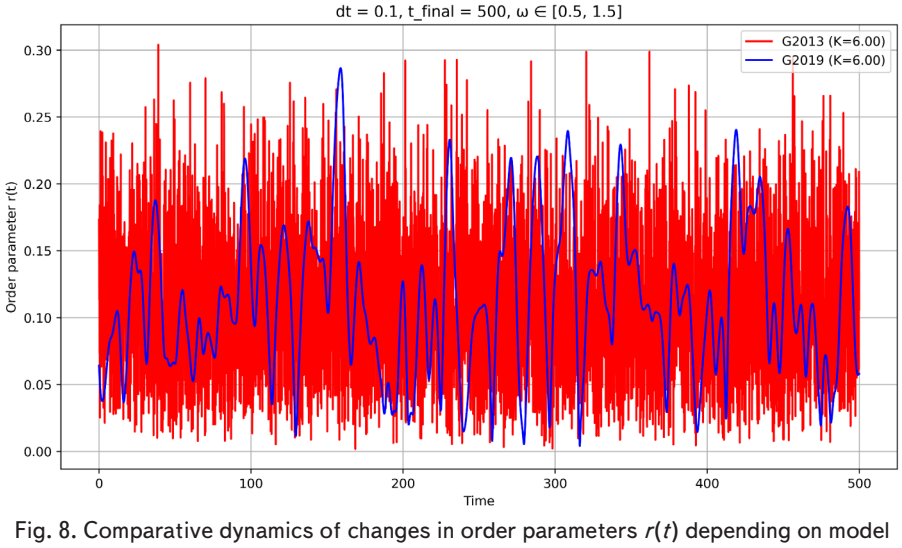

Fig. 8. Comparative dynamics of changes in order parameters $r(t)$ depending on model time of strongly connected components of two graphs G2013 and G2019 at $K = 6$

Table 3

Estimated SCC synchronization rates of two graphs G2013 and G2019 at $K = 6$

Indicator	G2013	G2019
SCC size	89	60
Spectral gap λ_2	19.913342	0.497646
Coupling force K	6.000000	6.000000
Critical coupling strength K_C	0.100435	4.018918
r_{max}	0.304108	0.286693
Time r_{max}	39.000000	158.900000
Start of the transition zone $r(t)$	0.173155	0.064093
End of the transition zone $r(t)$	0.304108	0.286693
Start of the transition zone t	0.000000	0.000000
End of the transition zone t	39.000000	158.900000
Synchronization rate Δr	0.003358	0.001401

At $K = 6$, both networks are formally under a supercritical mode but the behavior of the networks under conditions of strong interaction differs significantly. According to Table 3, in the SCC of G2013, the value of the synchronization order $r(t)$ increases to 0.3041, and the time to reach the maximum is reduced to 39 steps. At the same time, In the SCC of G2019, the maximum order parameter r_{max} is 0.2867, and the time increases to 158.9 steps ($r_{max} = 125.1$ at $K \approx K_C$, Table 2). This indicates that the G2013 network not only reaches the synchronous state faster but also demonstrates higher stability and coherence of dynamics with increasing interaction intensity.

The synchronization rate Δr in G2013 is 0.003358, which is more than twice as high as the similar indicator for the G2019 network, where Δr is only 0.001401. Given that both networks operate under a supercritical mode, the difference in dynamic response is explained solely by topological characteristics. In particular, G2013 has a high spectral gap, which ensures fast coordination of oscillation phases throughout the network. While G2019, despite the same coupling strength, demonstrates the effect of local coordination delay, which is a consequence of insufficient connectivity and a weak topological framework. The results indicate that the G2013 network has features of a stable centralized structure with the potential for effective global coordination, while G2019 is fragmented and vulnerable to the loss of key couplings.

From the perspective of the operational model, the 2013 TFP network tends to be hub-and-spoke, while the 2019 TFP network acquires the properties of a point-to-point model. In addition, a comparison of the results given in Tables 1–3 confirms the need to take into account not only the intensity of couplings K, but also the structural integration of the network, i.e., a high λ_2 index, when forming strategies for its development. It can be concluded that the structure of the network is a determining factor in the ability to synchronize, and only increasing the strength of couplings without topological reconstruction does not ensure the proper functioning of the railroad system.

6. Results of applying the method of analyzing the speed of transfer of car flows in a train formation plan: discussion

Our results of devising the method for analyzing the speed of transfer of car flows in a train formation plan make it possible to assess the dynamic properties of the transportation model from the point of view of the speed of transfer of car flows at the macro level of the functioning of the system for organizing freight cars into trains.

The application of the constructed scheme of the method (Fig. 4) and the simulation make it possible to compare the dynamic properties of the operating transportation system in the period between 2013 and 2019. The proposed formalization of the method reflects the dynamics of coordination not through the time of physical passage of trains in the network but through the ability of the system for organizing car flows into trains to quickly form a coherent state. For this purpose, our work introduced an indicator of the average increase in the order parameter in the transitional section of the modeling according to the Kuramoto model, which interprets the speed of coordination. This makes it possible to distinguish TFP networks with the same level of coherence but different speeds of its achievement. This procedure is key to comparing different versions of the train formation plan taking into account stochastic modeling conditions and provides an adequate interpretation of the transfer rate of car flows through the $r(t)$ dynamics over time. This forms a consistent approach

for comparison with topological PFT metrics, such as the spectral gap λ_2 and the critical coupling strength K_C, which determine the presence of threshold states in the network and its resistance to disturbances.

Comparison of the eigenvalues of the coupling strength of each SCC of the G2013 and G2019 graphs demonstrates systematic differences between the subnetworks (Fig. 5). In the G2013 network, the coupling strength is close to the critical threshold, which indicates relative structural stability, while in the G2019 network, the eigenvalue of the coupling strength is orders of magnitude smaller than the critical one, which indicates greater decentralization. Under these conditions, the average growth rate Δr is larger in the G2013 network, but local, rather than global, coherence is achieved, which increases the vulnerability to breaks in individual couplings and worsens the global coherence of the state of the entire network. This is confirmed by calculating $\lambda_2^{2013} \approx 19.913342$ and $\lambda_2^{2019} \approx 0.497646$, where the difference between the spectral gaps reaches two orders of magnitude, and the time to reach the maximum $r_{\max}$ in the G2019 SCC is significantly longer at comparable maximum values (Table 1).

Under the regime near the critical threshold ($K \approx K_C$), the behavior of the networks diverges even more noticeably (Fig. 6). For the G2013 TFP network, during the transition from the intrinsic value of the coupling strength $K_{SCC}^{G2013} = 0.0866$ to the critical value $K_C^{G2013} \approx 0.10$, the time to reach the maximum of the order parameter was reduced by almost half from 411.6 (Table 1) to 256 steps (Table 2), and $r_{\max}$ itself increased from 0.194367 to 0.216829. In parallel, the average growth rate Δr in the transition region increased from 0.000149 to 0.000729, which is interpreted as a sharp transition to more global coherence upon reaching the threshold. For the G2019 network, upon reaching the critical coupling strength $K_C^{G2019} \approx 4.02$, a decrease in $r_{\max}$ from 0.264661 to 0.171119 is observed and there is no significant gain in the time to reach the peak of 124.7 versus 125.1 steps. At the same time, the average rate Δr in the transition region increases from 0.000378 to 0.000636, but in combination with a very small spectral gap $\lambda_2^{2019} \approx 0.497646$, this indicates an insufficient network core for the propagation of coherence. Under the supercritical regime (at $K = 6$), the G2013 network not only reaches the synchronous state faster but also demonstrates higher stability and coherence of dynamics with increasing intensity of interactions (Table 3).

Phase analysis in a wide range of coupling strength values confirms the low ability to achieve global synchronization for both SCC networks of TFP (Fig. 7). The set of observations makes it possible to interpret the G2013 network as a structure closer to the hub-and-spoke type with a higher potential for global coordination, while the G2019 network demonstrates signs of a decentralized routing model with fragmentation and increased sensitivity to local violations of the integrity of the couplings. From a practical point of view, this means that it is the structural integration that determines the ability of the network to quickly coordinate actions and only increasing the strength of interactions without reconfiguring the framework does not provide the required level of coherence. Accordingly, when devising changes to the TFP, it is advisable to purposefully strengthen the core connectivity, increase the spectral gap, and minimize weak components that disrupt the propagation of coordinated ones.

The advantage of our study compared to works [3, 7, 9, 13, 22] is that for the first time the speed of transfer of car flows in the PFT was interpreted as the network coordination speed. In addition, it was quantitatively measured by the dynamics of the order parameter over time in coupling with the spectral gap of the Laplacian. Unlike [10, 16, 18, 19], an integrated approach was applied that combines the dynamics of the Kuramoto model on PFT graphs, the construction of phase diagrams of the dependence of the order parameters r on the model time, as well as spectral analysis of the largest strongly coupled components. This contributed to the improvement of the quality of the assessment of the structural and dynamic efficiency of the PFT network and provided an opportunity to compare alternative versions of the PFT and operating scenarios from the perspective of the dynamics of transportation processes.

The limitations of our study relate primarily to model assumptions, under which the TFP network is reduced to oscillatory dynamics with a phase variable without explicit consideration of queues, infrastructure constraints, and processing capabilities of stations, which affects the speed of propagation of car flows. Using this approach, it is possible to quickly determine the current transportation models in the system, assess the dynamic capabilities of the current transportation plan, and compare them. The disadvantages of the study include the lack of the ability to determine the real physical speed of car movement in the system. For such studies, it is necessary to build mathematical models that will take into account the specificity of transportation process at the micro level.

Conditions for the practical application of our results are the importance of taking into account not only the intensity of couplings but also the structural integration of the network, i.e., a high indicator when forming strategies for its development. It can be concluded that the structure of the network is a determining factor in the ability to synchronize, and only increasing the strength of couplings without topological reconstruction does not ensure the proper functioning of the car flow organization system.

Further development of our research is to study the internal spatial structure of SCC graphs of TFP networks and to identify local concentrations of synchronized activity. This will make it possible to proceed to studying the internal cluster organization of these components and identifying dense subsets of stations with similar phase behavior. In the future, it is important to detail the influence of individual stations and TFP network assignments on the coherence of the network. This will make it possible to comprehensively assess the influence of individual stations and TFP assignments on the dynamic properties of different networks.

7. Conclusions

1. We have determined the structure of the method for analyzing the speed of carriage flow propagation in a train formation plan, which includes seven consecutive stages from the selection of the most strongly connected component of the TFP graph to modeling the synchronization processes under different modes of the coupling strength K. Within the formalization of the method, the nodes in the TFP graph are interpreted as technical oscillator stations. Such oscillators perform the functions of coordinating the intensity of carriage flow propagation according to the corresponding TFP assignments, where their phases describe the state of coordination with other technical stations of the network. The evolution of the phases is described by the equations of the Kuramoto model with normalization of the coupling strength for a correct comparison of different topologies of TFP networks.

The integration of the Kuramoto model with spectral analysis for assessing the network's ability to synchronize has been justified. The structure of the method combines spectral, dynamic, and architectural analyses, which make it possible to interpret the speed of coordination of the railroad network operation through the rate of growth of the order parameter, spectral gap, and critical coupling strength. Based on the obtained indicators, it is proposed to interpret centralized hub-and-spoke models as more synchronized, and decentralized point-to-point models as less resistant to coherence.

2. Based on a comparative analysis of the speed of carriage traffic propagation when changing the topology of the TFP network over the period from 2013 to 2019, the change in the structural and dynamic efficiency of the TFP network was investigated using the formalization of the proposed method. It was found that the largest strongly connected component of the graph G2013 is characterized by a high ability to global synchronization, where the spectral gap $\lambda_2 = 19.91$, the critical coupling strength $K_C = 0.10$, and the maximum order parameter $r_{\max} = 0.304$, while for G2019 a low level of integration is observed, where the spectral gap $\lambda_2 = 0.50$, the critical coupling strength $K_C = 4.02$, $r_{\max} = 0.287$ and network fragmentation. The limited ability of TFP networks to global phase integration has been proven, which even when expanding the similarity threshold does not lead to complete coordination of phase behavior. It was found that the PFT network in 2019 demonstrates a loss of systemic coherence, which is typical of decentralized point-to-point transportation networks. This indicates a transformation of the operating model from a centralized hub-and-spoke in 2013 to a more decentralized point-to-point in 2019, which demonstrates fragmentation and local coherence. Our results showed that the ability of the PFT network to synchronize the direction depends on its topological structure. It was found that the PFT network reacts differently to disturbances in different years. Therefore, when building predictive models for transportation analysis with the identification of bottlenecks in the network, it is important to take into account the graph structure of PFT.

Conflicts of interest

The authors declare that they have no conflicts of interest in relation to the current study, including financial, personal, authorship, or any other, that could affect the study, as well as the results reported in this paper.

Funding

The study was conducted without financial support.

Data availability

The data will be provided upon reasonable request.

Use of artificial intelligence

The authors confirm that they did not use artificial intelligence technologies when creating the current work.

References

1. Strong, J. S. (2024). Operating innovation in North American railroads: Activist investors and precision scheduling railroading. Case Studies on Transport Policy, 15, 101164. https://doi.org/10.1016/j.cstp.2024.101164
2. Butko, T., Prokhorchenko, A., Golovko, T., Prokhorchenko, G. (2018). Development of the method for modeling the propagation of delays in noncyclic train scheduling on the railroads with mixed traffic. Eastern-European Journal of Enterprise Technologies, 1 (3 (91)), 30–39. https://doi.org/10.15587/1729-4061.2018.123141
3. Li, B., Jiang, S., Zhou, Y., Xuan, H. (2023). Optimization of train formation plan based on technical station under railcar demand fluctuation. Journal of Industrial and Production Engineering, 40 (6), 448–463. https://doi.org/10.1080/21681015.2023.2221699
4. Frisch, S., Hungerländer, P., Jellen, A., Lackenbucher, M., Primas, B., Steininger, S. (2022). Integrated freight car routing and train scheduling. Central European Journal of Operations Research, 31 (2), 417–443. https://doi.org/10.1007/s10100-022-00815-3
5. Butko, T., Prokhorov, V., Chekhunov, D. (2017). Devising a method for the automated calculation of train formation plan by employing genetic algorithms. Eastern-European Journal of Enterprise Technologies, 1 (3 (85)), 55–61. https://doi.org/10.15587/1729-4061.2017.93276
6. JSC "Ukrainian railways". Available at: https://www.uz.gov.ua/cargo_transportation Last accessed: 12.08.2025
7. But'ko, T., Prokhorchenko, A. (2013). Investigation into Train Flow System on Ukraine's Railways with Methods of Complex Network Analysis. American Journal of Industrial Engineering, 1 (3), 41–45.
8. Zhang, X., Zhu, T. (2023). Emergence of synchronization in Kuramoto model with general digraph. Discrete and Continuous Dynamical Systems – B, 28 (3), 2335–2390. https://doi.org/10.3934/dcdsb.2022172
9. Daganzo, C. F., Geroliminis, N. (2008). An analytical approximation for the macroscopic fundamental diagram of urban traffic. Transportation Research Part B: Methodological, 42 (9), 771–781. https://doi.org/10.1016/j.trb.2008.06.008
10. Wang, Y., Yu, X., Guo, J., Papamichail, I., Papageorgiou, M., Zhang, L. et al. (2022). Macroscopic traffic flow modelling of large-scale freeway networks with field data verification: State-of-the-art review, benchmarking framework, and case studies using METANET. Transportation Research Part C: Emerging Technologies, 145, 103904. https://doi.org/10.1016/j.trc.2022.103904
11. de Jong, G., Vierth, I., Tavasszy, L., Ben-Akiva, M. (2012). Recent developments in national and international freight transport models within Europe. Transportation, 40 (2), 347–371. https://doi.org/10.1007/s11116-012-9422-9
12. Butko, T., Muzykin, M., Prokhorchenko, A., Nesterenko, H., Prokhorchenko, H. (2019). Determining the Rational Motion Intensity of Train Traffic Flows on the Railway Corridors with Account for Balance of Expenses on Traction Resources and Cargo Owners. Transport and Telecommunication Journal, 20 (3), 215–228. https://doi.org/10.2478/ttj-2019-0018

13. Szymula, C., Bešinović, N., Nachtigall, K. (2024). Quantifying periodic railway network capacity using petri nets and macroscopic fundamental diagram. Transportation Research Part C: Emerging Technologies, 158, 104436. https://doi.org/10.1016/j.trc.2023.104436
14. Khomenko, Y., Okorokov, A., Matsiuk, V., Zhuravel, I., Pavlenko, O. (2025). Revealing the causes of delays at transit points along an intermodal grain supply chain. Eastern-European Journal of Enterprise Technologies, 4 (3 (136)), 40–50. https://doi.org/10.15587/1729-4061.2025.338166
15. Helbing, D. (2001). Traffic and related self-driven many-particle systems. Reviews of Modern Physics, 73 (4), 1067–1141. https://doi.org/10.1103/revmodphys.73.1067
16. Saw, V.-L., Chung, N. N., Quek, W. L., Pang, Y. E. I., Chew, L. Y. (2019). Bus bunching as a synchronisation phenomenon. Scientific Reports, 9 (1). https://doi.org/10.1038/s41598-019-43310-7
17. Kuramoto, Y.; Araki, H. (Ed.) (1975). Lecture Notes in Physics, International Symposium on Mathematical Problems in Theoretical Physics. Vol. 39. New York: Springer-Verlag, 420.
18. Rodriguez, M., Fathy, H. K. (2022). Distributed Kuramoto Self-Synchronization of Vehicle Speed Trajectories in Traffic Networks. IEEE Transactions on Intelligent Transportation Systems, 23 (7), 6786–6796. https://doi.org/10.1109/tits.2021.3062178
19. Fretter, C., Krumov, L., Weihe, K., Müller-Hannemann, M., Hütt, M.-T. (2010). Phase synchronization in railway timetables. The European Physical Journal B, 77 (2), 281–289. https://doi.org/10.1140/epjb/e2010-00234-y
20. Yoon, S., Sorbaro Sindaci, M., Goltsev, A. V., Mendes, J. F. F. (2015). Critical behavior of the relaxation rate, the susceptibility, and a pair correlation function in the Kuramoto model on scale-free networks. Physical Review E, 91 (3). https://doi.org/10.1103/physreve.91.032814
21. Wang, Y., Doyle, F. J. (2013). Exponential Synchronization Rate of Kuramoto Oscillators in the Presence of a Pacemaker. IEEE Transactions on Automatic Control, 58 (4), 989–994. https://doi.org/10.1109/tac.2012.2215772
22. Wang, W., Du, W., Liu, K., Tong, L. (2022). The Evolution of China's Railway Network (CRN) 1999-2019: Urbanization Impact and Regional Connectivity. Urban Rail Transit, 8 (2), 134–145. https://doi.org/10.1007/s40864-022-00168-9
23. Peng, S., Lu, J., Jiang, B., Zhu, J. (2024). Synchronization of high-dimensional Kuramoto-oscillator networks with variable-gain impulsive coupling on the unit sphere. Nonlinear Analysis: Hybrid Systems, 54, 101536. https://doi.org/10.1016/j.nahs.2024.101536
24. Lei, L., Han, W., Yang, J. (2021). Kuramoto model with correlation between coupling strength and natural frequency. Chaos, Solitons & Fractals, 144, 110734. https://doi.org/10.1016/j.chaos.2021.110734
25. Böhle, T., Kuehn, C., Thalhammer, M. (2021). On the reliable and efficient numerical integration of the Kuramoto model and related dynamical systems on graphs. International Journal of Computer Mathematics, 99 (1), 31–57. https://doi.org/10.1080/00207160.2021.1952997
26. Gherardini, S., Gupta, S., Ruffo, S. (2018). Spontaneous synchronisation and nonequilibrium statistical mechanics of coupled phase oscillators. Contemporary Physics, 59 (3), 229–250. https://doi.org/10.1080/00107514.2018.1464100
27. McGraw, P. N., Menzinger, M. (2007). Analysis of nonlinear synchronization dynamics of oscillator networks by Laplacian spectral methods. Physical Review E, 75 (2). https://doi.org/10.1103/physreve.75.027104
28. O'Kelly, M. E., Park, Y. (2023). Contrasts in Sustainability between Hub-Based and Point-to-Point Airline Networks. Sustainability, 15 (20), 15111. https://doi.org/10.3390/su152015111
29. Sabhahit, N. G., Khurd, A. S., Jalan, S. (2024). Prolonged hysteresis in the Kuramoto model with inertia and higher-order interactions. Physical Review E, 109 (2). https://doi.org/10.1103/physreve.109.024212
30. Arenas, A., Díaz-Guilera, A., Kurths, J., Moreno, Y., Zhou, C. (2008). Synchronization in complex networks. Physics Reports, 469 (3), 93–153. https://doi.org/10.1016/j.physrep.2008.09.002